

Copper – Manganese – Tin

Nathalie Lebrun

Introduction

Sn based soldering alloys are good candidates for microelectronics applications and are widely used in establishing electrical contacts between metals, of which one is invariably copper.

The Cu rich part of the ternary system Cu-Mn-Sn has been extensively studied and experimental data are reported in Table 1.

Only one ternary phase MnCu_4Sn , called τ , has been observed and disagreements are noticed concerning its composition.

There is also disagreement in the experimental observations of solubility of Mn in the β phase of the Cu-Sn binary system. According to [1933Ver, 1955Ada], the β phase disappears at Mn contents of about 5 to 10 mass%, respectively, whereas [1942Car, 1953Fun, 1953Val, 1973Mey, 1987Leo] show a much wider β phase region, up to 30 or 40 mass% Mn. [1942Car] mentioned that β phase is stable at only elevated temperature but it can be retained above 625°C by quenching.

[1954Bla] established experimentally partial polythermal sections for 5 to 20 mass% Mn. It was shown that the higher is Mn concentration, the lower is solid solubility of Sn in (Cu), varying above 600°C from 15.8 to 5.8 mass% when Mn concentration increases up to 20 mass%. Polythermal sections at 85 and 75 mass% Cu, and at 2 mass% Mn have been constructed experimentally by [1987Leo] and [1985Dri, 1987Leo], respectively. The liquidus and solidus curves measured by [1990Boc] are in good agreement with those reported previously. From diffusion couple measurements, [2004Liu] calculated isopleths at 16.7 at.% Mn and 16.7 at.% Sn, which disagree with those reported previously. From thermodynamic description, [2004Mie] calculated isopleths which fit well with experimental data of [1942Car, 1953Fun, 1953Val, 1954Bla, 1987Leo].

Isothermal sections at 350 to 750°C have been reported by [1953Fun, 1987Leo, 2004Liu]. Very good agreement of the results of [1953Fun] and [1987Leo] has been observed, in contradiction with data [2004Liu] who observed a $A2/B2$ order-disorder transition. The isothermal sections of the latter work have also been calculated using a CALPHAD method and present a congruent melting of the ternary phase τ in disagreement with experimental work [1987Leo] suggesting formation of τ via a eutectoid reaction involving the β phase. Through thermodynamic considerations, [2004Mie] calculated isothermal sections which are in good agreement with those reported in the literature.

In the compilation of [1995Vil], a liquidus surface done by [1955Ada] has been reported. [2004Mie] calculated a partial liquidus surface in the Cu rich corner which is not in agreement with the one given by [1955Ada].

A complete thermodynamic description of the ternary system in the Cu rich part has been performed by [2004Mie] using ThermoCalc software.

[1961Die, 1979Cha, 1979Dri] undertook a review of the system Cu-Mn-Sn.

Binary Systems

The binary system Cu-Mn is taken from [2005Tur]. No reliable data on Cu-Sn and Mn-Sn are available in the literature after [Mas2]. Only the Cu rich part of the Cu-Sn phase diagram was re-investigated by [2004Liu] which concluded the presence of a two stage, second order reaction $A2 > B2 > D0_3$ in the bcc phase region, rather than a two-phase equilibrium between the disordered $A2$ bcc phase and the ordered $D0_3$ bcc phase as reported before. The existence of this second order transition has been detected by DSC technique at 649°C on a Cu-16.9 at.% Sn. This result has been confirmed using high temperature electron diffraction technique showing a $D0_3$ ordered structure at 550°C and a $B2$ ordered structure at 675°C in a Cu-16.1 at.% Sn alloy. These experimental results have been supported by a CALPHAD method in which the Gibbs energy of the bcc phase is described by the two-sublattice model in order to take into account the

A2/B2 ordering reaction. No significant modifications have been reported by this previous study. Consequently, the phase diagram proposed by [Mas2] is accepted in this assessment. Mn–Sn phase diagram is taken from [Mas2].

Solid Phases

All crystallographic data for the unary, binary and ternary phases are reported in Table 2.

A ternary phase has been detected by several authors with different referring: δ' [1954Bla] and θ [1953Fun, 1987Leo]. Various composition have been attributed: MnCu_5Sn_2 [1933Ver], MnCu_2Sn [1954Bla] and MnCu_4Sn [1961Gla, 1968Joh, 1973Mey, 1987Leo, 2004Liu].

MnCu_2Sn was investigated by [1954Bla, 1972Gel, 1981Uhl]. It was found that this alloy melts at around 657°C and its $L2_1$ structure exits down to 497°C. Two structure changes have been observed [1961Tag]. Using annealed samples, it was shown that the stable phase MnCu_2Sn at room temperature is not cubic. [1942Car] suggested a hexagonal structure.

The binary β phase presents a large domain of existence inside the ternary system. This solid solution is ordered and stable at temperatures higher than 400°C. It can be retained at room temperature through quenching [1963Oxl]. In fact, its domain strongly depends on the annealing treatment of the alloys. Using quenched samples, [1942Car] stipulated that β consists of a body-centered structure with a face-centered superlattice and the lattice parameter was estimated to be $a = 616.08$ pm at a composition of MnCu_2Sn . This value agrees well with the one reported later in [1953Val, 1972Gel, 1977Mac]. [1973Mey] determined the lattice parameters inside the domain of the β phase and found a small variation of the lattice parameter varying from $a = 606.6 \pm 0.3$ to 617.6 ± 0.9 pm). The same author detected a lower temperature MnCu_4Sn type structure in all the alloys, the lattice parameter was estimated to be $a = 698.2 \pm 0.3$ pm in agreement with the value of $a = 698.8 \pm 0.3$ given by [1961Gla].

The most reliable composition of the ternary compound τ seems to be MnCu_4Sn which has been retained in this assessment.

[2004Liu] suggested that τ presents a small solubility range.

Invariant Equilibria

Invariant equilibria and reaction scheme are presented in Table 3 and Fig. 1. The values of the U_6 , U_7 , U_8 and E_1 given in the table are estimated from the diagram given by [1955Ada] and should be considered as tentative. For the ternary reactions U_4 and U_5 , their positions have been deduced from the calculated partial liquidus surface presented by [2004Mie]. The phase compositions in other ternary reactions were directly deduced from Fig. 2 and should be also considered as tentative.

Liquidus, Solidus and Solvus Surfaces

[1995Vil] mentioned the liquidus surface constructed by [1955Ada] who found a narrow region of the primary β phase. Recently [2004Mie] undertook a thermodynamic description of the ternary system and reported a partial calculated liquidus surface in the Cu rich corner. There is a clear disagreement concerning the stability of the β phase. According to [1955Ada], the β phase disappears at Mn content of about 10 mass% whereas other studies [1942Car, 1953Fun, 1953Val, 1972Mey, 1987Leo] show a much wider β phase region reaching up to 30 or 40 mass% Mn. These last experimental results were confirmed by the thermodynamic calculation done by [2004Mie]. However, the β phase region is not allowed to extend to such high tin content [1942Car]. Consequently, the phase region has been estimated in this assessment on the base of the partial liquidus surface proposed by [2004Mie]. The sequence of the ternary reactions proposed in the Cu rich corner by [1955Ada] have not been retained in this assessment since recent thermodynamic evaluation suggested different four-phase equilibria which are more reliable. The monovariant curve proposed by [1955Ada] in the Mn rich corner is not acceptable as different solid phases participate in the equilibria. The equilibria have been changed and a sequence of two ternary reactions has been proposed. Moreover, the equilibrium $L + \text{MnSn}_2 + \eta + (\beta\text{Sn})$ is more likely of eutectic type since the

solubilities of Mn and Cu in (β Sn) are negligible. Then instead of the U_7 reaction proposed by [1955Ada], it was replaced by a E reaction.

The accepted liquidus surface, in accordance with the binary systems, is presented in Fig. 2 with the accepted data of [2004Mie] in the Cu rich corner and the schematic liquidus projection of [1955Ada] in the Sn corner. Tentative liquidus and isothermal curves have been indicated by dashed lines on the drawing. The calculated isothermal curves from [2004Mie] at 1000 and 900°C reproduce well those of [1955Ada]. Taking into account Alkemade's rule, position of some invariant points have been modified in Fig. 2.

Isothermal Sections

Several isothermal sections have been constructed in the Cu rich corner [1953Fun, 1987Leo, 2004Liu]. All the experimental works are in good agreement. However the isothermal sections suggested by [2004Liu] have not been retained in this assessment since some inconsistencies have been observed with the polythermal sections proposed by [1954Bla, 1987Leo]. Indeed, the latter works detected a maximum temperature of 610°C for decomposition of the τ phase, whereas [2004Liu] suggested its congruent melting at about 680°C using CALPHAD calculation. [2004Mie] calculated few isothermal sections in the Cu rich corner which are in quite good agreement with the experimental ones. Some of them are reported in Figs. 3 to 7. The diagrams have been slightly changed in accordance with the accepted binary diagrams.

Temperature – Composition Sections

Partial polythermal sections have been reported in the literature [1954Bla, 1987Leo, 1990Boc], the experimental data are in good agreement. The β phase decomposes eutectoidally into (γ Mn,Cu) and the ternary phase τ [1987Leo, 1954Bla]. The temperature of the eutectoid reaction varies considerably with the Mn content, and has a maximum at 610°C and 13 mass% Mn [1954Bla]. These results are in contradiction with the calculated partial isopleths [2004Liu] who proposed a congruent melting of τ at around 680°C. Since no experimental data supported the calculations, this latter work has not been accepted in this assessment. [2004Mie] also calculated isopleths which agree reasonably well with the experimental data [1953Fun, 1985Dri, 1987Leo, 1990Boc]. Some inconsistencies were observed with the polythermal sections proposed by [1955Ada] who did not detect the ternary phase τ .

Some examples of isopleths are reported in Figs. 8 to 13, in accordance with the binary edges. In order to be in agreement with the isothermal sections at 450 and 550°C, slight modifications have been done in the isopleth at 15 mass% Mn (Fig. 11) since the equilibrium $\tau + (\beta\text{Mn}) + \text{Mn}_3\text{Sn}$ exists. The modifications are indicated as dashed lines.

Thermodynamics

The enthalpies of formation in the β region have been measured by [1972Mey] ranging from 383 to 933 J·mol⁻¹ closely the composition MnCu_2Sn .

Notes on Materials Properties and Applications

Brief details of some experimental works on materials properties are reported in Table 4.

Certain Cu–Mn–Sn alloys were ferromagnetic especially when the binary β phase was present. The estimated value of the magnetization σ to be about 60.8 Am²·kg⁻¹ [1983Bus] and 68.7 Am²·kg⁻¹ [1975Wac] at 530°C for a MnCu_2Sn alloy. These values are in the same range order as those reported previously by [1953Val]. For the same composition, [1942Car] observed a maximum value of $\sigma = 76.65 \text{ Am}^2 \cdot \text{kg}^{-1}$ at 660°C. [1914Heu] also measured the magnetic saturation which is found to be maximal (107 Am²·kg⁻¹) for a composition of $\text{Mn}_2\text{Cu}_9\text{Sn}$. The Curie temperature of MnCu_2Sn alloy has been extrapolated at 357°C [1981Uhl, 1982Uhl] where a decreasing of the magnetization occurs. This extrapolated value of the Curie temperature is far from the one calculated by [1975Wac] who found a value of 240°C. The ferromagnetic moment has been estimated to be $\mu_{\text{OO}} = 4.00 \mu_{\text{B}}$ for a quenching temperature of 645°C. This value is in agreement with those of [1942Car, 1963Oxl]. On molten Cu–Sn alloys with Mn

impurities (25 at.%), [1975Gue] found a linear variation of the reciprocal magnetic susceptibility with temperature, varying from 350 to 900 g-atom·cm⁻³ in the temperature range 400 to 1400°C. These values are lower than those reported by [1975Wac] for the same composition range.

Tempering quenched Cu alloys with 5-20 mass% Mn and 4-14 mass% Sn, results in extreme brittleness, owing to unfavorable distribution of the τ phase [1954Bla]. Cold working the alloys before tempering leads to more homogeneous texture, *i.e.* dispersed particles τ in a (Cu) matrix. Thus tensile strengths of 35-38 tons/in² with elongations of 10-20% can be obtained.

The electrical properties of some Cu based alloys and thin evaporated films containing additions of Mn and Sn have been measured by [1990Boc]. The electrical resistivity has been found for the alloys greater than values for the films. The electrical resistivity increases regularly from about 40·10⁸ Ohm m at Cu-25%Mn to 83·10⁸ Ohm m at Cu-25%Sn [1984Boc].

Miscellaneous

In the case of amorphous MnCu₂Sn, the only annealing temperature which produced ferromagnetism was 200°C [1982Tay]. At all temperatures this phase was mixed with a major second phase Mn₂Cu₃Sn.

The magnitude and sign of the hyperfine field in MnCu₂Sn has been measured at -196°C by means of Mössbauer spectroscopy and found to be +200 ± 10 kOe [1972Gel].

Low temperature specific heat measurements were performed on MnCu₂Sn and show a soft phonon distribution leading to an Einstein temperature of about -220°C [1991Fra].

References

- [1914Heu] Heusler, F., "Study of the Magnetisation of the Manganese Alloys", *Z. Anorg. Chem.*, **88**, 185-188 (1914) (Experimental, Magn. Prop., 3)
- [1933Ver] Veroe, J., "Equilibrium Conditions of Further Alloyed Bronses, III. Cu-Mn-Sn Alloys Rich in Cu", *Mitt. Berg. Huett. Abt. Ung. Hochschule Berg. Forstwesen Sopron*, **5**, 128-155 (1933) (Experimental, Phase Diagram, 16)
- [1942Car] Carapella, L.A., Hultgren, R., "The Ferromagnetic Nature of the Beta Phase in the Copper-Manganese-Tin System", *Trans. Amer. Inst. Min. Met Eng.*, **147**, 232-244 (1942) (Crys. Structure, Experimental, Magn. Prop., Phase Diagram, 36)
- [1953Fun] Funk, C.W., Rowland, J.A., "α Solid-Solution Area of the Cu-Mn-Sn System", *Trans. Am. Inst. Min. Metall. Pet. Eng.*, **197**, 723-725 (1953) (Experimental, Phase Diagram, Phase Relations, 18)
- [1953Val] Valentiner, S., "Into Knowledge of the Copper-Manganese-Tin System" (in German), *Z. Metallkd.*, **44**, 59-64 (1953) (Crys. Structure, Experimental, Magn. Prop., Phase Relations, 11)
- [1954Bla] Blade, J.C., Cuthbertson, J.W., "The Structure and Mechanical Properties of Copper-Manganese-Tin Alloys", *J. Inst. Met.*, **82**, 17-24 (1954) (Mechan. Prop., Phase Diagram, 14)
- [1955Ada] Adachi, M., Sasakai, Y., "Invesigation of the Ternary Equilibrium Diagram of Copper-Manganese-Tin System", *Trans. Mining Metall. Aluminium Assoc.*, **12**, 591-594 (1955) quoted in [1995Vil]
- [1961Die] Dies, K., "Manganese Bronses", *Metall*, **15**(12), 1161-1172 (1961) (Review, Experimental, 8)
- [1961Gla] Gladyshevskii, E.I., Kripyakevich, P.I., Teslyuk, M.Y., Zarechnyuk, O.S., Kuz'ma, Y.B., "Crystal Structures of Some Intermetallic Compounds", *Sov. Phys.-Crystallogr.*, **6**, 207-208 (1961), translated from *Kristallografiya*, 1960, **6**(2), 267 (Review, Crys. Structure, 11)
- [1961Tag] Taglang, P., Fournier, "On the Transformations of the Alloy MnSnCu₂", *J. Phys. Radium*, **22**, 295-297 (1961) (Experimental, 7)
- [1963Oxl] Oxley, D.P., Tebble, R.S., Williams, K.C., "Heusler Alloys", *J. Appl. Phys.*, **34**, 1362-1364 (1963) (Crys. Structure, 13)

- [1968Joh] Johnston, G., “Neutron Diffraction Investigation of Ternary Manganese Alloys”, *At. Energy Aust.*, **11**, 18-24 (1968) (Crys. Structure, 15)
- [1972Gel] Geldart, D.J.W., Campbell, C.C.M., Pothier, P.J., Leiper, W., “Moessbauer Effect Study of the Hyperfine Fields at the Sn Sites in Cu_2MnSn ”, *Canad. J. Phys.*, **50**, 206-212 (1972) (Experimental, Crys. Structure, 20)
- [1972Mey] Meyers, M.A., Hepworth, M.T., “The Enthalpies of Formation of Ferromagnetic Cu-Mn-Sn Alloys”, *Met. Trans. AIME*, **3**(9), 2544-2547 (1972) (Experimental, Thermodyn., 2)
- [1973Mey] Meyers, M.A., Ruud, C.O., Barrett, C.S., “Observations on the Ferromagnetic β Phase of the Cu-Mn-Sn System”, *J. Appl. Crystallogr.*, **6**, 39-41 (1973) (Crys. Structure, Magn. Prop., 10)
- [1975Gue] Günther, H.H., Wachtel, E., Gerold, V., “Magnetic Properties of Molten Cu-Sn Alloys with Mn Impurities” (in German), *Physica*, **80B**, 473-491 (1975) (Experimental, Magn. Prop., 15)
- [1975Wac] Wachtel, E., Kruse, H., “Magnetic Investigations in Copper-Tin-Manganese Alloys with 25 at.% Mn (Solid and Liquid State)”, *Z. Metallkd.*, **66**(7), 431-437 (1975) (Experimental, Magn. Prop., 3)
- [1977Mac] MacDonald, R.A., Stager, C.V., “Magnetic Properties of $(\text{Ni}_x\text{Cu}_{1-x})_2\text{MnSn}$ ”, *Canad. J. Phys.*, **55**(17), 1481-1484 (1977) (Experimental, Crys. Structure, Magn. Prop., 9)
- [1979Cha] Chang, Y.A., Neumann, J.P., Mikula, A., Goldberg, D., “Cu-Mn-Sn”, *INCRA Monograph Series 6 Phase Diagrams and Thermodynamic Properties of Ternary Copper-Metall Systems*, NSRD, Washington, **6**, 549-557 (1979) (Crys. Structure, Phase Diagram, Review, 18)
- [1979Dri] Drits, M.E., Bochvar, N.R., Guzei, L.S., Lysova, E.V., Padezhnova, M.P., Rokhlin, L.L., Turkina, N.I., “Cu-Mn-Sn”, in “*Binary and Multicomponent Copper-Base Systems*”, Nauka, Moscow, 169-170 (1979) (Phase Diagram, Review, 9)
- [1981Uhl] Uhl, E., “Magnetic Properties of New Heusler Alloys $(\text{Cu}_{1-x}\text{Co}_x)_2\text{MnSn}$ ”, *J. Magn. Magn. Mater.*, **25**, 221-227 (1981) (Magn. Prop., 34)
- [1982Tay] Taylor, R.C., Tsuei, C.C., “Amorphous Heusler Alloys: The Effect of Annealing on Structure and Magnetic and Transport Properties”, *Solid State Commun.*, **41**(6), 503-506 (1982) (Crys. Structure, Magn. Prop., 11)
- [1982Uhl] Uhl, E., “Magnetism in Mixed Heusler Alloys $(\text{Ni}_{1-x}\text{Cu}_x)_2\text{MnSn}$ ”, *Monatsh. Chem.*, **113**(3), 275-284 (1982) (Magn. Prop., 26)
- [1983Bus] Buschow, K.H.J., van Engen, P.G., Jongebreur, R., “Magneto-Optical Properties of Metallic Ferromagnetic Materials”, *J. Magn. Magn. Mater.*, **38**, 1-22 (1983) (Magn. Prop., Optical Prop., 23)
- [1984Boc] Bochvar, N.R., Vigdorovich, V.N., Leonova, N.P., Lysova, E.V., “Resistivity of Alloys of Cu-Mn-Ge, Cu-Mn-Sn and Cu-Ge-Sn Systems” (in Russian), *Metalloved. Term. Obrab. Met.*, **2**, 61-64 (1984) (Experimental, Electr. Prop., 9)
- [1985Dri] Drits, M.E., Bochvar, N.R., Lysova, E.V., Leonova, N.P., “A Study of the Nature of Component Interaction in Copper-Based Alloys Containing Manganese, Tin, and Germanium”, in “*Stable and Metastable Phase Equilibria in Metallic Systems*”, Nauka, Moscow, 55-59 (1985) (Experimental, Phase Diagram, 5)
- [1987Leo] Leonova, N.P., Bochvar, N.R., Lysova, E.V., “Phase Equilibria in Copper-Rich Cu-Mn-Sn Alloys”, *Russ. Metall.*, **4**, 204-206 (1987) translated from *Izv. Akad. Nauk SSSR, Met.*, **4**, 203-205 (1987) (Experimental, Phase Diagram, 5)
- [1990Boc] Bochvar, N., Lysova, E.V., “Correlation between Phase Diagrams and Electrical Properties of Cu-Alloys and Films Deposited via Evaporation in Vacuum”, *User Aspects of Phase Diagrams*, Proceedings Conf., Petten, Netherlands June 1990; Hayes, F.H. (Ed.), UMIST, Manchester (UK), 180-184 (1990) (Electr. Prop., Experimental, Phase Diagram, Phase Relations, 5)

- [1990Goe] Goedecke, T., “Physical Measurements on Copper-Manganese Alloys. III. Influence of the Quenching Temperature on the Electrical Resistance and on the Dilatation of the Alloys” (in German), *Z. Metallkd.*, **81**, 826-835 (1990) (Experimental, Phase Diagram, Phase Relations, 17)
- [1991Fra] Fraga, G.L.F., Brandao, D.E., Sereni, J.G., “Specific Heat of $X_2\text{MnSn}$ ($X = \text{Co}, \text{Ni}, \text{Pd}, \text{Cu}$), $X_2\text{MnIn}$ ($X = \text{Ni}, \text{Pd}$), and Ni_2MnSb Heusler Compounds”, *J. Magn. Magn. Mater.*, **102**(1/2), 199-207 (1991) (Experimental, 27)
- [1993Gok] Gokcen, N.A., “The Cu-Mn (Copper-Manganese) System“, *J. Phase Equilib.*, **14**(1), 76-83 (1993) (Review, Phase Diagram, Crys. Structure, Thermodyn., 52)
- [1995Vil] Villars, P., Prince, A., Okamoto, H., *Handbook of Ternary Alloy Phase Diagrams*, ASM Int., Materials Park, OH, **Vol. 8**, 9694-9707 (1995) (Phase Diagram)
- [2004Liu] Liu, X.J., Wang, C.P., Ohnuma, I., Kainuma, R., Ishida, K., “Experimental Investigation and Thermodynamic Calculation of the Phase Equilibria in the Cu-Sn and Cu-Sn-Mn Systems”, *Metal. Mat. Trans. A*, **35A**, 1641-1654 (2004) (Experimental, Calculation, Phase Diagram, 55)
- [2004Mie] Miettinen, J., “Thermodynamic Description of the Cu-Mn-Sn System in the Copper-Rich Corner”, *Calphad*, **28**, 71-77 (2004) (Assessment, Calculation, Phase Diagram, Thermodyn., 28)
- [2005Tur] Turchanin, M., Agraval, P., Gröbner, J., Matusch, D., Turkevich, V., “Cu-Mn (Copper - Manganese)”, MSIT Binary Evaluation Program, in *MSIT Workplace*, Effenberg G. (Ed.), MSI, Materials Science International Services GmbH, Stuttgart; Document ID: 20.14136.1.20 (2005) (Crys. Structure, Phase Diagram, Phase Relations, Thermodyn., Assessment, 25)

Table 1: Investigations of the Cu-Mn-Sn Phase Relations, Structures and Thermodynamics

Reference	Method/Experimental Technique	Temperature/Composition/Phase Range Studied
[1933Ver]	Thermal and microscopic methods	400-1100°C / Cu_3Sn -Mn with 5 to 15 mass% Mn
[1942Car]	X-ray diffraction	640 to 715°C / Cu-based alloys with 0-40 mass% Mn and 0-30 mass% Sn
[1953Fun]	Metallographic analysis	350 to 750°C / Cu rich corner with 0 to 20 mass% Mn and 0 to 25 mass% Sn
[1953Val]	X-ray diffraction	MnCu_2Sn
[1954Bla]	Metallographic analysis, DTA	400 - 700°C / Cu alloys with 5-20 mass% Mn and 4-14 mass% Sn
[1961Tag]	X ray diffraction	MnCu_2Sn
[1968Joh]	X-ray and neutron diffraction	MnCu_2Sn
[1972Gel]	X ray diffraction	Annealed at 640°C / MnCu_2Sn
[1972Mey]	Liquid-metal solution calorimetry	25°C / $\sim \text{MnCu}_2\text{Sn}$
[1973Mey]	X-ray analysis	25°C after annealing at 600°C for 3 h / MnCu_2Sn and 50.1-64.8 at.% Cu with 24.8-32.3 at.% Mn and 8.7-25.1 at.% Sn
[1977Mac]	X ray diffraction	MnCu_2Sn

Reference	Method/Experimental Technique	Temperature/Composition/Phase Range Studied
[1985Dri]	Metallography	400 - 1200°C / Cu rich based alloys with 2 mass% Mn and 2-10 mass% Sn
[1987Leo]	microhardness measurements, DTA, metallographic analysis,	300 to 1000°C / Cu-Mn-Sn up to 30 mass% Sn and 30 mass% Mn
[1990Boc]	DTA, microscopic and X-ray analysis	700 - 1100°C / 2 mass% Mn and 0-25 mass% Cu
[2004Liu]	Diffusion couple method, DSC, electron diffraction and high temperature X-ray diffraction techniques	550 - 700°C / Cu based alloys with 0-30 at.% Mn and 0-30 at.% Sn

Table 2: Crystallographic Data of Solid Phases

Phase/ Temperature Range [°C]	Pearson Symbol/ Space Group/ Prototype	Lattice Parameters [pm]	Comments/References
(γ Mn,Cu)	<i>cF4</i> <i>Fm$\bar{3}m$</i> Cu	$a = 362.63$ $a = 375$	[Mas2] Melting point [1993Gok] at $x = 0.04$ [V-C2] at $x = 0.80$ [V-C2]
(γ Mn) 1138 - 707		$a = 386$	at $x = 1$ [Mas2]
(Cu) < 1084.62		$a = 361.46$	at $x = 0$ [Mas2]
(δ Mn) 1246 - 1138	<i>cI2</i> <i>Im$\bar{3}m$</i> W	$a = 308.0$	[Mas2]
(β Mn) 1087 - 707	<i>cP20</i> <i>P4₁32</i> β Mn	$a = 631.52$	[Mas2]
(α Mn) < 707	<i>cI58</i> <i>I$\bar{4}3m$</i> α Mn	$a = 891.26$	at 25°C [Mas2]
(γ Sn)	<i>tI2</i> ? γ Sn	$a = 370$ $c = 337$	at 25°C, 9.0 GPa [Mas2]
(β Sn) 231.9681 - 13	<i>tI4</i> <i>I4₁/amd</i> β Sn	$a = 583.18$ $c = 318.18$	at 25°C [Mas2]

Phase/ Temperature Range [°C]	Pearson Symbol/ Space Group/ Prototype	Lattice Parameters [pm]	Comments/References
(α Sn) < 13	<i>cF8</i> <i>Fd$\bar{3}m$</i> C (diamond)	$a = 648.92$	[Mas2]
β , Cu ₁₇ Sn ₃ 798 - 586	<i>cI2</i> <i>Im$\bar{3}m$</i> W	$a = 302.61$	from 13.1 to 16.5 at.% Sn and <i>A2</i> type structure [Mas2, 2004Liu]
γ , Cu ₃ Sn(h) ~755 - 520	<i>cF16</i> <i>Fm$\bar{3}m$</i> or <i>F$\bar{4}3m$</i> BiF ₃ or CuHg ₂ Ti	$a = 611.76 \pm 0.10$	from 15.5 to 27.5 at.% Sn [2004Liu] from 16.5 to 27.9 [Mas2, V-C2] <i>D0₃</i> type structure [2004Liu]
γ' phase ~755 - 574	<i>hP8</i> ? Na ₃ As	$a = 428.1$ $c = 784.2$	from 15.5 to 23 at.% Sn [2004Liu] <i>B2</i> type structure [2004Liu] metastable, martensitic form of quenched γ
ϵ , Cu ₃ Sn(r) < 676	<i>oC80</i> <i>Cmcm</i> Cu ₃ Sn	$a = 552.9 \pm 0.8$ $b = 477.5 \pm 0.6$ $c = 432.3 \pm 0.5$	24.5 to 25.9 at.% Sn and Cu ₃ Sn [Mas2, V-C2]
ζ , Cu ₁₀ Sn ₃ 640 - 582	<i>hP26</i> <i>P6₃</i> Cu ₁₀ Sn ₃	$a = 733.0 \pm 0.4$ $c = 786.4 \pm 0.5$	20.3 to 22.5 at.% Sn and Cu ₁₀ Sn ₃ at 603°C [Mas2, V-C2]
δ , Cu ₄₁ Sn ₁₁ 582 - ~350	<i>cF416</i> <i>F$\bar{4}3m$</i> Cu ₄₁ Sn ₁₁	$a = 1796.46 \pm 0.06$	20 to 21 at.% Sn and Cu ₄₁ Sn ₁₁ [Mas2, V-C2]
η , Cu ₆ Sn ₅ (h) 415 - 186	<i>hP4</i> <i>P6₃/mmc</i> NiAs	$a = 419.2 \pm 0.2$ $c = 503.7 \pm 0.2$	43.5 to 44.5 at.% Sn and [Mas2, V-C2]
η' , Cu ₆ Sn ₅ (r) < 189	<i>h**</i>		44.8 to 45.5 at.% Sn, ordered form with superlattice based on η [Mas2]
γ_1 , MnCu ₅ ≤ 410	<i>c**</i>	-	[1990Goe]
ϵ_2 , MnCu ₃ ≤ 450	<i>c**</i>	-	[1990Goe]
γ_3 (Cu-Mn phase) ≤ 700	<i>c**</i>	-	[1990Goe]

Phase/ Temperature Range [°C]	Pearson Symbol/ Space Group/ Prototype	Lattice Parameters [pm]	Comments/References
Mn ₃ Sn < 984	<i>hP8</i> <i>P6₃/mmc</i> Ni ₃ Sn	<i>a</i> = 567 <i>c</i> = 453	[V-C2] Mn ₁₉ Sn ₆ in [2004Mie]
Mn ₂ Sn < 884	<i>hP6</i> <i>P6₃/mmc</i> InNi ₂	<i>a</i> = 437.7 ± 0.1 <i>c</i> = 550.7 ± 0.1	[V-C2]
MnSn ₂ < 549	<i>tI12</i> <i>I4/mcm</i> Al ₂ Cu	<i>a</i> = 665.9 ± 0.3 <i>c</i> = 544.7 ± 0.3	[V-C2]
* τ, MnCu ₄ Sn	<i>cF24</i> <i>F43m</i> AuBe ₅	<i>a</i> = 698.8 ± 0.3	[1961Gla]
* MnCu ₂ Sn(h) 657 - 497	<i>cF16</i> <i>Fm3m</i> BiF ₃	<i>a</i> = 617.6 ± 0.9	[1973Mey]
* MnCu ₂ Sn(r) < 497	<i>hP2</i> <i>P6/mmc</i> Mg	<i>a</i> = 285.2 <i>c</i> = 401.4	[1954Bla]

Table 3: Invariant Equilibria

Reaction	<i>T</i> [°C]	Type	Phase	Composition (at.%)		
				Cu	Mn	Sn
L + (δMn) ⇌ (βMn) + (γMn,Cu)	1029-1000	U ₁	L	3.80	79.80	16.40
L + (βMn) ⇌ Mn ₃ Sn + (γMn,Cu)	984-900	U ₂	L	4.10	76.50	19.4
L + (γMn,Cu) ⇌ β + Mn ₃ Sn	798-750	U ₃	L	62.94	28.90	8.16
L + Mn ₃ Sn ⇌ β + Mn ₂ Sn	700-650	U ₄	L	49.89	28.90	21.21
L + β ⇌ Mn ₂ Sn + γ	650-600	U ₅	L	50.91	22.31	26.78
L + γ ⇌ Mn ₂ Sn + ε	~ 510	U ₆	L	39.84	17.44	42.72
L + ε ⇌ Mn ₂ Sn + η	415-400	U ₇	L	12.22	6.02	81.76
L + Mn ₂ Sn ⇌ η + MnSn ₂	400-231	U ₈	L	9.22	4.42	86.36
L ⇌ η + (βSn) + MnSn ₂	< 227	E ₁	L	0.46	0.46	99.08

Table 4: Investigations of the Cu-Mn-Sn Materials Properties

Reference	Method/Experimental Technique	Type of Property
[1914Heu]	Magnetometer	Magnetic properties
[1942Car]	Magnetometer	Magnetic properties
[1953Val]	Magnetometer	Magnetic properties
[1954Bla]	Hardness measurements	Tensile properties
[1963Oxl]	Standard Sucksmith technique	Magnetic properties
[1975Gue]	Susceptibility measurements	Magnetic properties
[1975Wac]	Susceptibility measurements	Magnetic properties
[1981Uhl]	Faraday magnetometer	Magnetic properties
[1982Uhl]	Faraday pendulum magnetometer	Magnetization and susceptibility coefficients
[1983Bus]	Spectroscopic technique, PAR vibrating sample magnetometer	Magnetization coefficient, magneto-optical Kerr rotation
[1984Boc]	Resistivity measurements	Electrical properties
[1990Boc]	Auger spectroscopy and electrical resistivity measurements	Electrical resistivity and electrical resistivity temperature coefficient

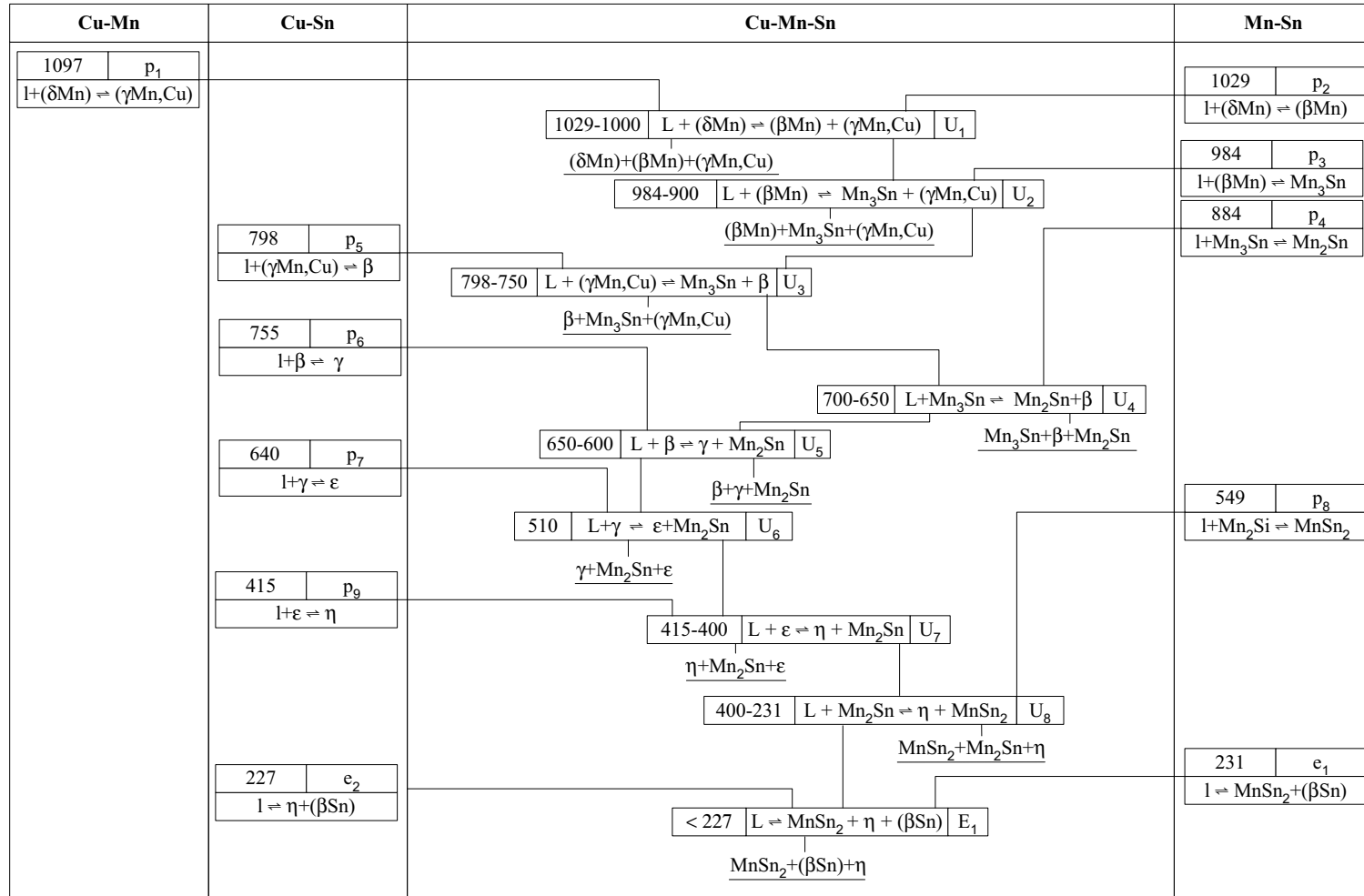


Fig. 1: Cu-Mn-Sn. Reaction scheme

Fig. 2: Cu-Mn-Sn.
Liquidus surface
projection

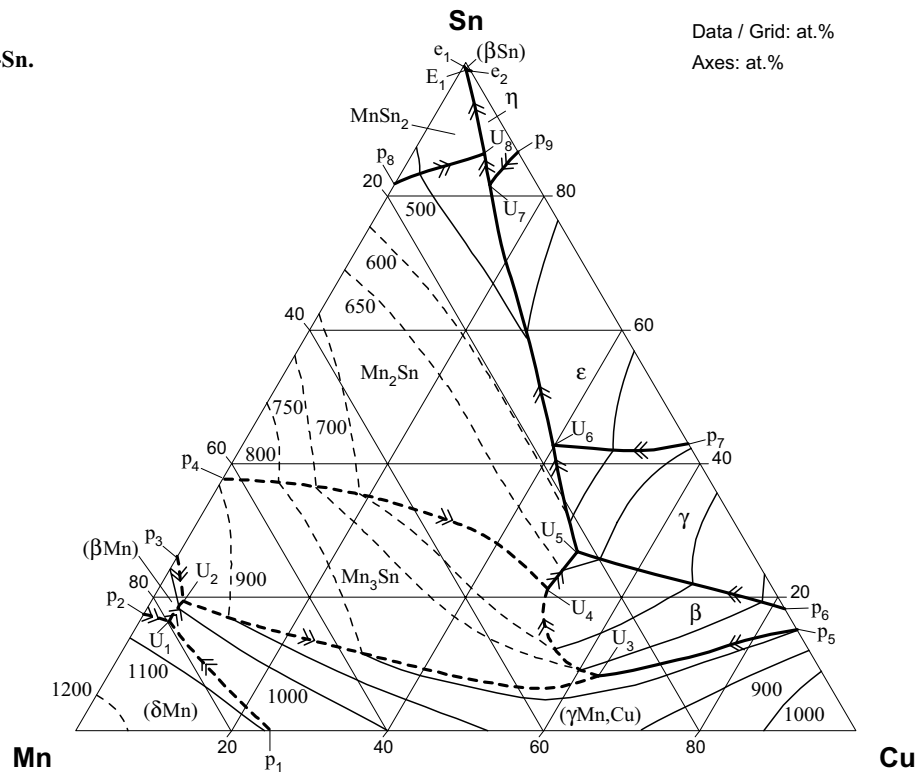


Fig. 3: Cu-Mn-Sn.
Isothermal section in
the Cu rich part at
750°C

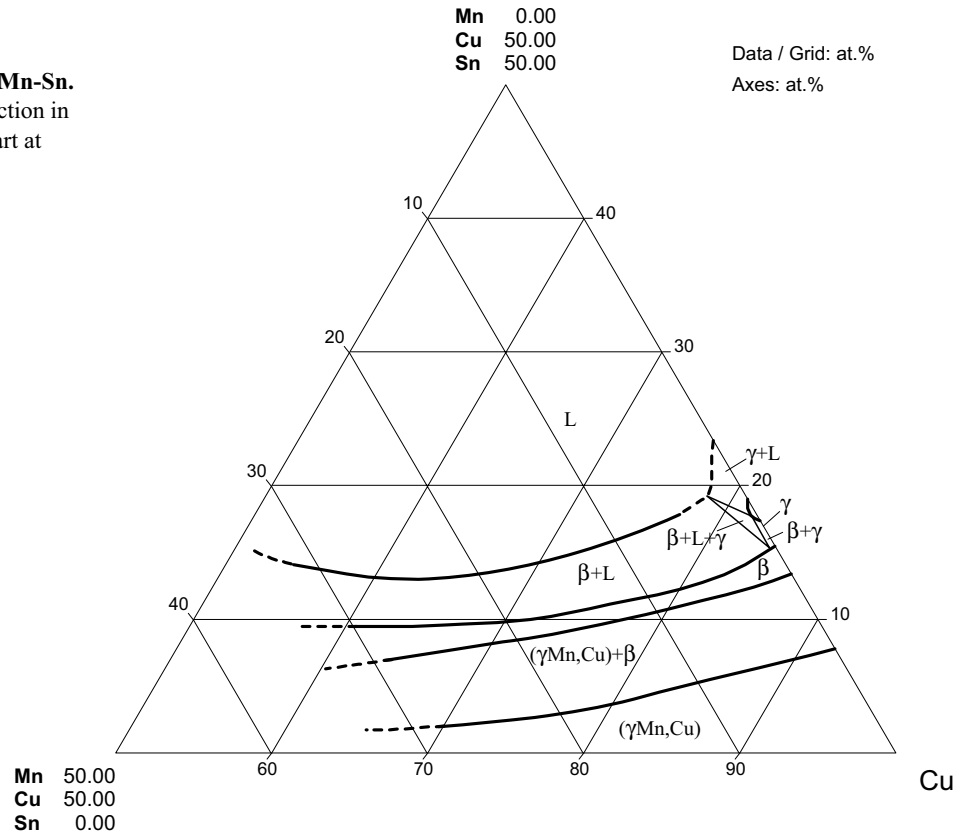


Fig. 4: Cu-Mn-Sn.
Isothermal section in
the Cu rich part at
700°C

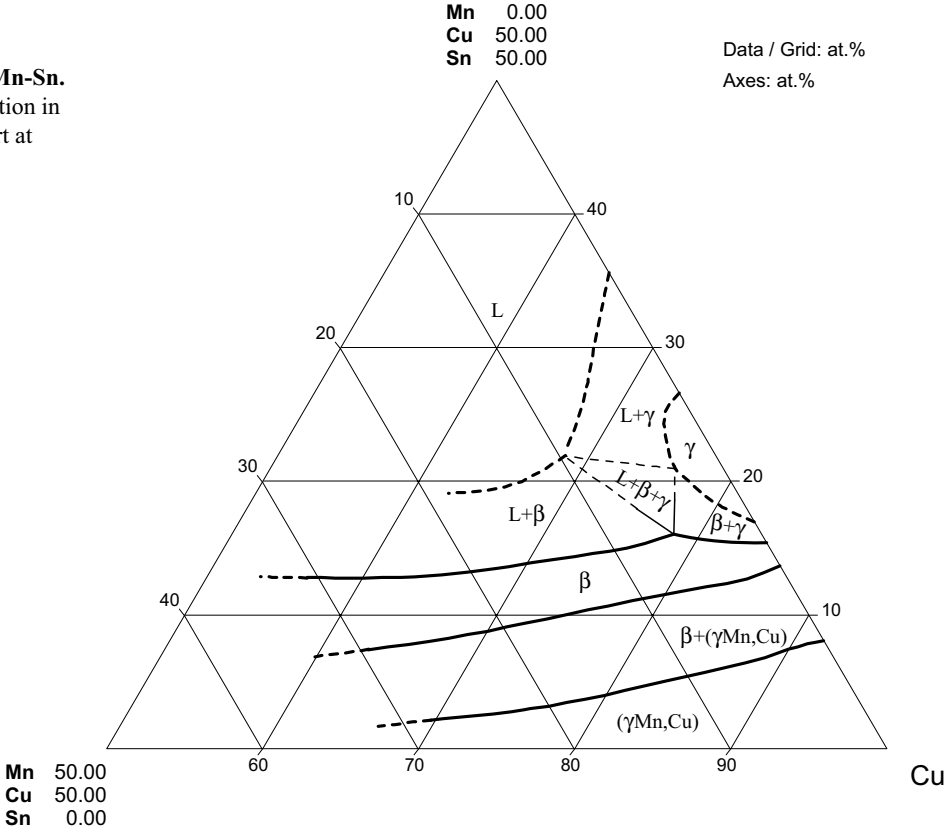


Fig. 5: Cu-Mn-Sn.
Isothermal section in
the Cu rich part at
650°C

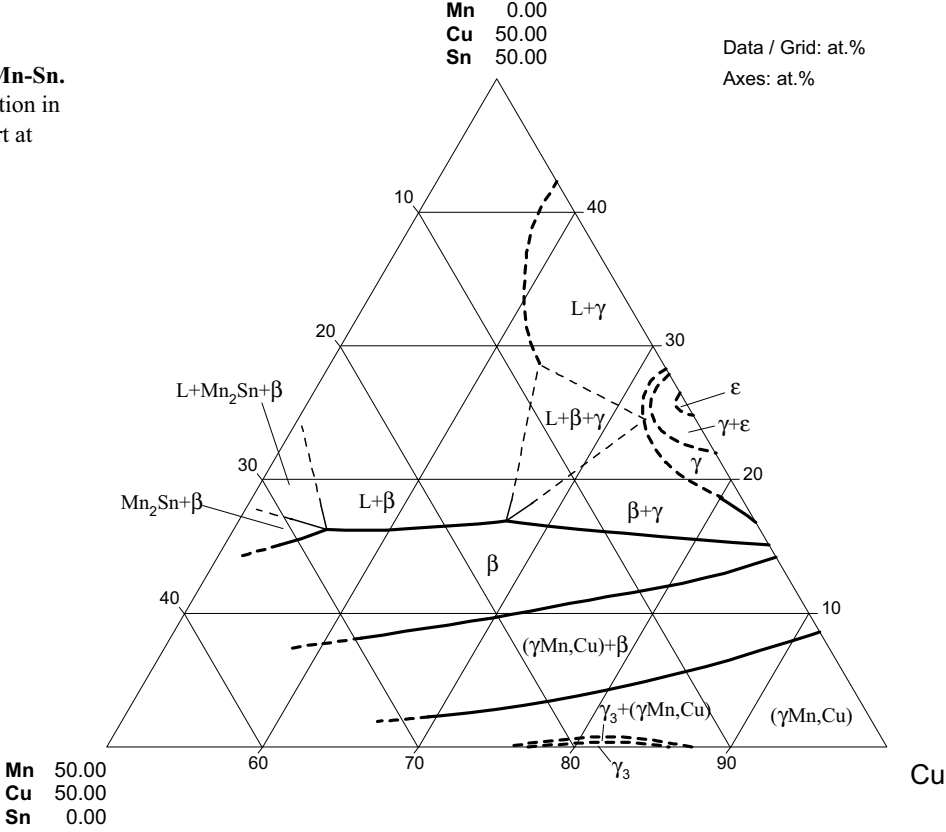


Fig. 6: Cu-Mn-Sn.
Calculated isothermal
section in the Cu rich
part at 550°C

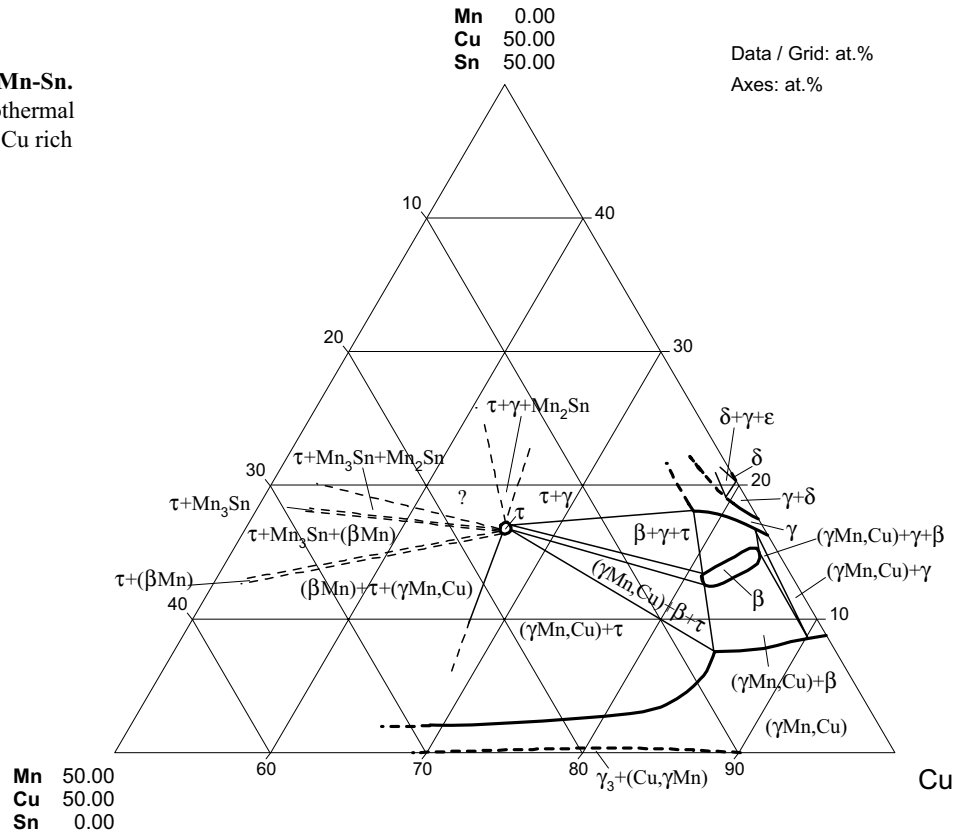


Fig. 7: Cu-Mn-Sn.
Calculated isothermal
section in the Cu rich
part at 450°C

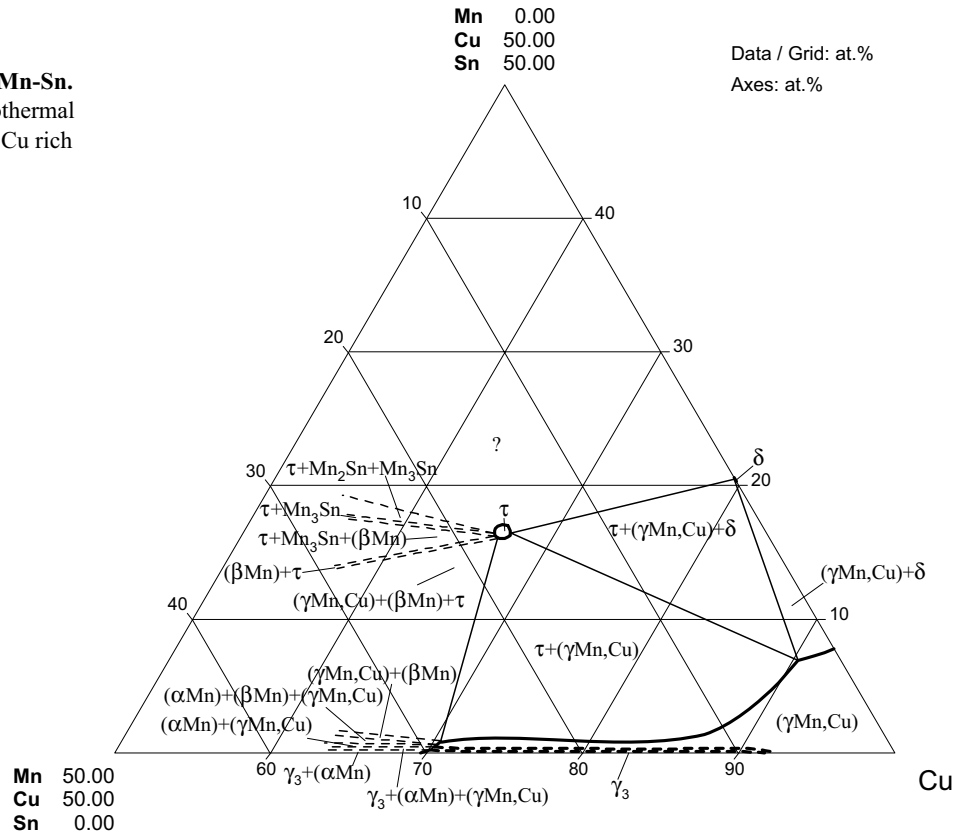


Fig. 8: Cu-Mn-Sn.
Isopleth at 2 mass%
Mn in the Cu rich
corner, plotted in at. %

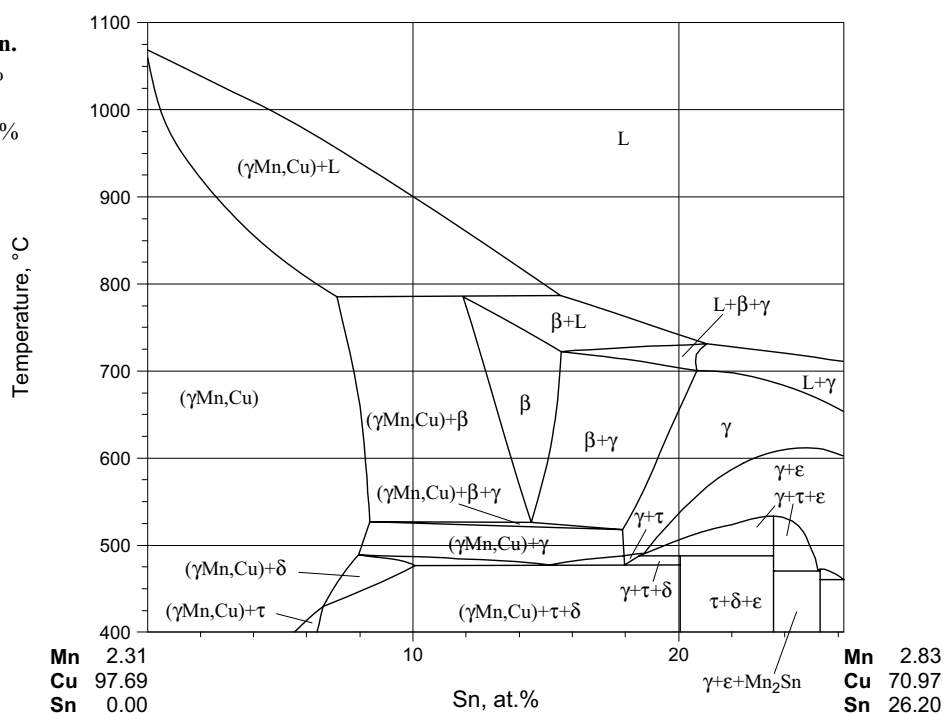


Fig. 9: Cu-Mn-Sn.
Isopleth at 5 mass%
Mn in the Cu rich
corner, plotted in at. %

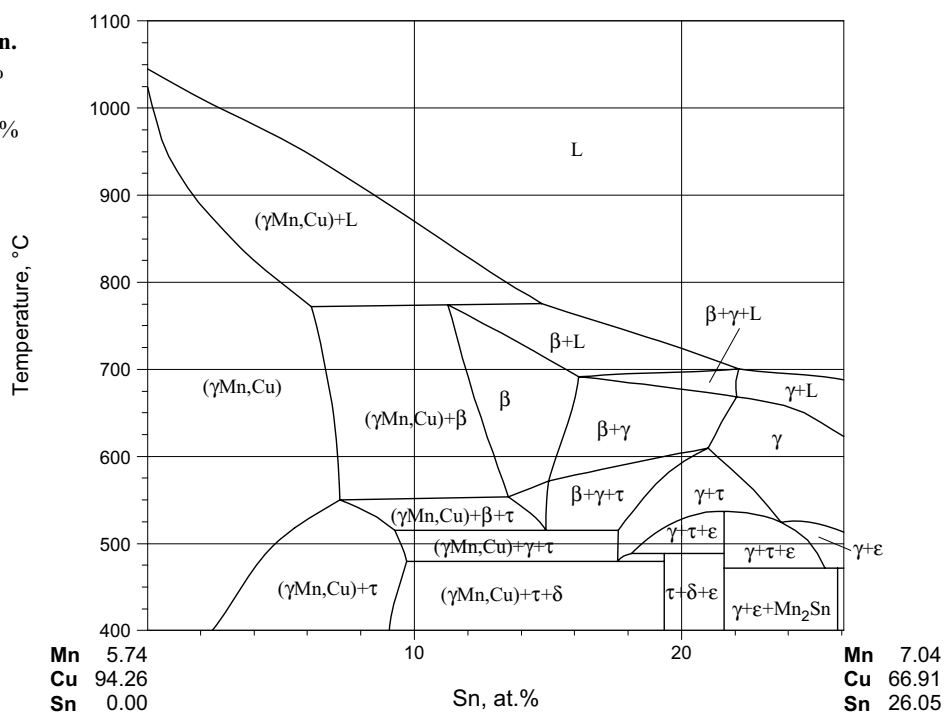


Fig. 10: Cu-Mn-Sn.
Isopleth at 10 mass%
Mn in the Cu rich
corner, plotted in at. %

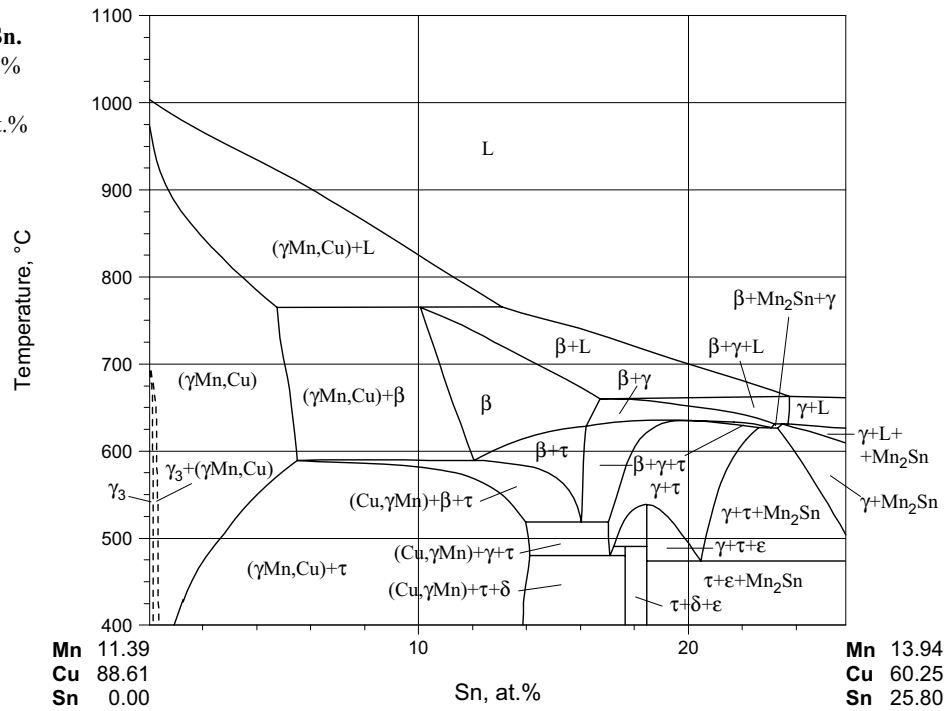


Fig. 11: Cu-Mn-Sn.
Isopleth at 15 mass%
Mn in the Cu rich
corner, plotted in at. %

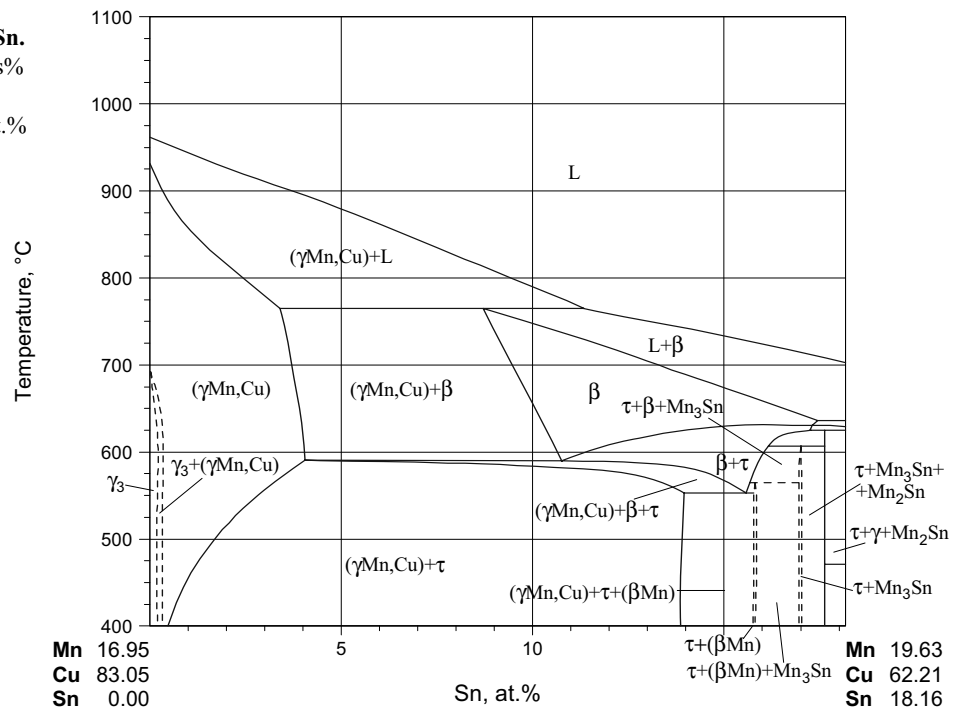


Fig. 12: Cu-Mn-Sn.
Isopleth at 85 mass%
Cu in the Cu rich
corner, plotted in at. %

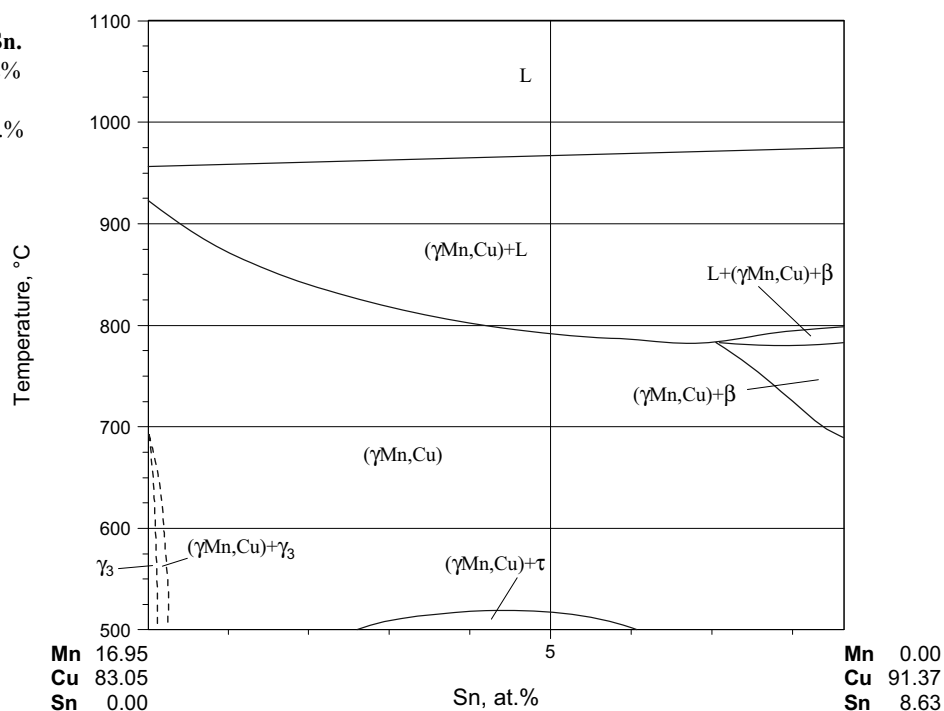


Fig. 13: Cu-Mn-Sn.
Isopleth at 75 mass%
Cu in the Cu rich
corner, plotted in at. %

